Available online at www.sciencedirect.com

ScienceDirect

Procedia CIRP 74 (2018) 674–678

www.elsevier.com/locate/procedia

10th CIRP Conference on Photonic Technologies [LANE 2018]

Inconel 718 laser welding simulation tool based on a moving heat source and phase change

Iñigo Hernando[a,]*, Mario Alfredo Renderos[a], Magdalena Cortina[a], Jose Exequiel Ruiz[a], Jon Iñaki Arrizubieta[a], Aitzol Lamikiz[a]

[a]*Dept. of Mechanical Engineering, University of the Basque Country, Plaza Torres Quevedo 1, Bilbao, 48013, Spain*

* Corresponding author. Tel.: +34-946-017-347 ; fax: +34-946-014-215. *E-mail address:* inigo.hernando@ehu.eus

Abstract

Modern aerospace industry demands the union of different Inconel 718 parts ensuring the quality of the joint. Therefore, in the present work a novel fiber laser welding model that considers wobbling strategy is developed. The heat source model definition and solid-liquid phase change phenomena are taken into account as bead is considered liquid zone during the melting, getting a robust-but-simple tool for prediction of bead and heat affected zone geometries depending on process parameters. One of the main drawbacks is the maximum welded bead width, which is limited by the beam spot. In order to overcome this handicap, wobbling strategy allows covering a wider area by combining elliptical and linear motions. Optimal relation between these orbital and translation speeds is defined for minimum overlap among consecutive wobble rings. Likewise, temperature rise at welded joint is estimated by existing and modified heat source models after relying on experimental validation.

Peer-review under responsibility of the Bayerisches Laserzentrum GmbH.

Keywords: laser welding; Inconel 718; wobbling; simulation

1. Introduction

Nickel-based alloys offer a good response against fatigue strength and corrosive environments in addition to thermal stability. These facts contribute these materials to comprise about 50% weight of aerospace engine. More specifically, Inconel 718 superalloy presents high strength due to its small γ'' and γ''' precipitates that are high in Ni [2], which makes it suitable for gas turbines components that have to deal with both structure supporting and chemical corrosion.

The joining of different parts must ensure mechanical properties that can withstand numerous flight work conditions. According to this, the manufacturing and subsequent analysis of the welded zones, which are subject to hard thermal changes during their formation, are essential for the components comply as a whole. Several welding techniques as Electron Beam Welding (EBW), Tungsten Plasma Arc Welding (PAW) or Inert Gas Tungsten Arc Welding (TIG) have traditionally been used for pieces union. In relation to them, Laser Beam Welding (LBW) is a recently developed welding method that offers a well concentrated heat source in addition to a good adaptability with automatized tooling machines [3].

Inconel 718 is susceptible to microffisures appearence in the Heat Affected Zone (HAZ) despite its good performance against weld solidification cracking [4], so it is primary to generate a narrow HAZ. In addition to this fact and regarding the equipments, laser tools can be simply fixtured and do not require vacuum chambers for their use [5], making LBW an emergent alternative to traditional systems as EBW.

The service level that a component can offer is subject to most vulnerable zones, which include the welds as they suffer a properties drop in comparison to the original material. Hence, aerospace industry has the need of develop robust predictive tools for arising welding techniques that produce the minimum impact as possible. Several authors as

Peer-review under responsibility of the Bayerisches Laserzentrum GmbH.
10.1016/j.procir.2018.08.045

Mazumder and Steen [5], Goldak [6], Swifthook [7] or Dowden [8] have proved the utility of creating heat source models that help products designing and fabrication processes.

In this work, a predictive model is developed and validated by experimental results in order to analyse the geometry of different Inconel 718 seams depending on the input parameters used in LBW process.

2. Materials and Experimental Procedure

Inconel 718 sheets of 2 mm thickness were chosen for this research as they are used in Tail Bearing Housings (TBH), which are structural components that both connect the engine with the wings of the aircraft and redirect the outgoing fuel from the gas turbine.

Table 1. Chemical composition (wt. %) of Inconel 718 [9]

Al	B	C	Co	Cr	Cu	Fe
0.55	0.004	0.054	0.28	18.60	0.05	18.60
Mn	Mo	Ni	P	S	Si	
0.24	3.03	52.40	<0.005	<0.002	0.06	
Ti	Nb	Ta	Bi	Pb	Ag	
0.98	4.89	<0.05	<0.00003	<0.0005	<0.0002	

The trials were executed by a Yb:YAG fiber laser source with a maximum power of 1 KW and 1070 nm wavelength. The laser spot on the surface of the workpiece is of 100 µm, so wobbling technique was employed for covering a wider area and creating a consistent weld seam. This method combines orbital and linear motions by rapid movements of the optical glasses that are located in the scanner.

In this work, a 900 µm diameter wobbling (d_w) was selected, which added to the laser spot diameter (d_s) gives a 1 mm heat source. Different powers from 350 W to 500 W were combined with 3 mm·s^{-1} and 5 mm·s^{-1} advancing speeds along x axis.

Fig. 1. Analysed test samples.

The thermal dilatations and contractions during the melting process may cause misalignment distortions in the weld zone. This defect could enhance the static stress concentration factor (k_t) at the limits of the weld bead, rising the stress that a piece should handle with. This factor is defined as the ratio between the maximum stress and the nominal stress at a specfic zone, thus, $k_t=\sigma_{max}/\sigma_{nom}$. The test samples were clamped for the trials in order to prevent stress peaks due to sudden geometry changes at the weld crown and root.

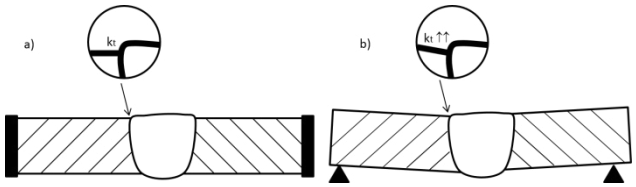

Fig. 2. (a) Result after clamping; (b) Non-clamped and misaligned trial.

For the purpose of avoiding excess energy supply for weld formation, a relation between feeding speed (v_f) and peripherical speed (v_p) was established. In this way, minimum overlap and no space between consecutive rings were obtained by equalizing the time spent for describing a ring (t_{loop}) and the one for advancing a ring width distance (t_{width}) (equations 1-3).

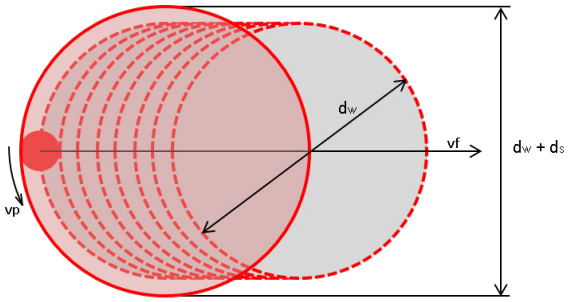

Fig. 3. Wobbling method schematic view.

$$t_{loop} = \frac{loop\ length}{v_p} \quad (1)$$

$$t_{width} = \frac{spot\ width}{v_f} \quad (2)$$

$$v_p = \frac{v_f * (loop\ length)}{spot\ width} \quad (3)$$

In order to create a protection atmosphere against oxidation and stabilize the laser welding process [10] , argon shielding gas was used. The protective gas flow rate was of 24 L·min^{-1} and introduced as it is shown in the scheme in Figure 4.

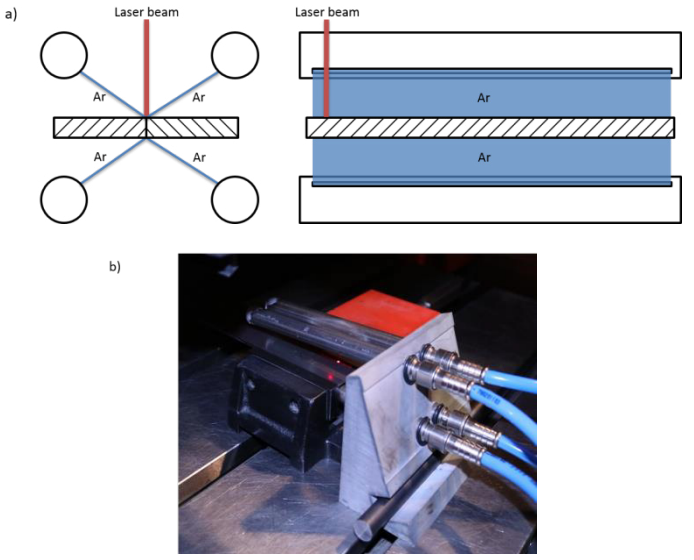

Fig. 4. (a) Argon shielding scheme; (b) Argon shielding tooling.

3. Analytical Model

The temperature distribution *T(x,y,z)[K]* induced by a moving laser heat source over a surface is defined in equation (4) [11] [12] .

$$T(x,y,z) = \int_{-\infty}^{\infty}\int_{-\infty}^{\infty} AI(x',y')W(x-x',y-y',z)dx'dy' \quad (4)$$

$$W = \frac{e^{\left[\frac{-v}{2\alpha}(x-x'+R)\right]}}{2\pi\lambda R} * \frac{1}{2}\left[1-\operatorname{erf}\left(\frac{R-vt}{2\sqrt{\alpha t}}\right)+e^{Rv/\alpha}\left(1-\operatorname{erf}\left(\frac{R+vt}{2\sqrt{\alpha t}}\right)\right)\right] \quad (5)$$

$$R = \sqrt{(x-x')^2+(y-y')^2+z^2} \quad (6)$$

Each point has a concrete temperature according to its absorptivity (A), applied power intensity (I), thermal conductivity (λ), thermal diffusivity (α) and the laser advancing speed (v).

The model used in this work is based on Matlab Laser Toolbox [13], which considers constant thermo-physical properties. Applying two-dimensional Fourier transform, the temperature field described in equation (4) is defined as in equation (7).

$$F_2\{T\} = F_2\{AI * W\} \leftrightarrow F_2\{T\} = AF_2\{I\}F_2\{W\} \leftrightarrow \tilde{T} = A\tilde{I}\tilde{W} \quad (7)$$

The temperatures estimation was fixed by taking into account variable conductivity, diffusivity and absorptivity of the material depending on obtained temperature increments through the thermal conduction process. The model represents the temperature field at each time step, and it finishes its calculus when there is no difference between two consecutive temperature fields (steady state). The properties of each point are heritated from its temperature of the previous time step.

Table 2. Temperature dependent material properties of Inconel 718 [14]

Temperature (K)	Density (kg m^{-3})	Specific heat (J kg^{-1} K^{-1})	Thermal conductivity (W m^{-1} K^{-1})
298	8190	435	8.9
373	8160	455	10.8
473	8118	479	12.9
573	8079	497	15.2
673	8040	515	17.4
773	8001	527	18.7
873	7962	558	20.8
973	7925	568	21.9
1073	7884	680	26.9
1173	7845	640	25.8
1273	7806	620	26.7
1373	7767	640	28.3
1443	7727	650	29.3
1609	7400	720	29.6
1673	7340	723	29.6
1773	7250	743	29.6
1873	7160	764	29.6

The absorbed laser power and its consequent effects on the materials final shape can be fairly predicted [8], so the absorptivity of a material is the basis for any heat transfer modeling [15]**.** While the absorptivity of Inconel 718 at room temperature is close to 0.3 [2], the absorption at the keyhole can be considered as complete, thus, it works as a blackbody [16]. For this reason, the model also considers a progressive absorptivity rise from 293 K (*A=0.3*) to the pure nickel vaporization temperature, thus, 3100 K (*A=1*).

Moreover, forced convection phenomena at top and bottom surfaces was applied for simulating the argon supply influence.

Regarding the laser power, the model simulates a circular heat source, so a relation between the power supplied in the wobbling experiments (*Preal*) and the model input (*Psim*) must be fixed considering the wobble ring and the circle areas (*Areal* and *Asim*, respectively). Whereas the trials are carried out by advancing rings that combine orbital and linear motions, the simulation introduces a single advancing circular filled surface. This assumption can be introduced when the intensity supplied by a ring and a circle are connected by a geometrical relation of their respective areas. This allows to make the problem less complex as the orbital movement is neglected.

Equalizing the laser beam surface intensity for both cases, *Psim=Preal*(Asim/Areal)*. In this case, *Asim/Areal=2.78*, thus, *Psim=2.78*Preal*.

$$A_{sim} = \frac{\pi(d_w+d_s)^2}{4} \quad (8)$$

$$A_{real} = \frac{\pi(d_w+d_s)^2}{4} - \frac{\pi(d_w-d_s)^2}{4} = \pi d_w d_s \quad (9)$$

The transience that the welding process has to deal with until reaching the stable stage relies on the properties change as the keyhole is generated and moved through the substrate. In this sense, it must be known that the steady state will be achieved if there is a minimum laser feeding speed that produces enough vapor able to get through the melting material in its pathway [17]

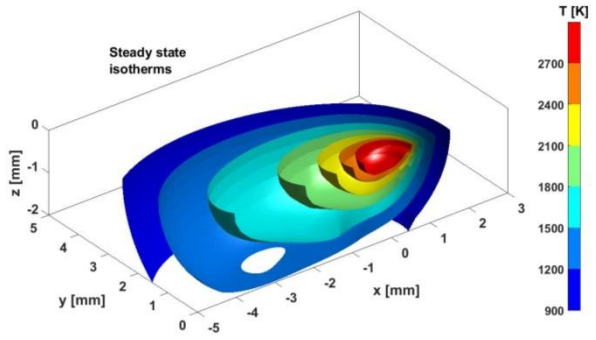

Fig. 5. Steady state temperatures for 500 W and 3 mm/s feeding speed.

The criterium for predicting the melted material dimensions is based on the Inconel 718 solidus temperature, thus, 1533 K. All the zones over this temperature are therefore considered as part of the weld seam.

4. Results and Discussion

The widths of the weld seams were measured on the surface and then compared with the temperature fields obtained by the analytical model. The results showed a less than 5% error between the trials and the simulations.

Table 3. Seam width measurements for different process parameters

Power (W)	Feeding speed ($mm \cdot s^{-1}$)	Simulated width (mm)	Measured width (mm)	Error (%)
350	3	2.224	2.202	1.00
350	5	2.024	1.951	3.74
400	3	2.464	2.473	0.36
400	5	2.142	2.043	4.85
450	3	2.704	2.662	1.58
450	5	2.424	2.365	2.49
500	3	2.944	3.001	1.90
500	5	2.584	2.509	2.99

5. Conclusion

The present research demonstrates that a high accuracy is obtained by comparing the real trials and the simulated seams from the used analytical model when the material properties as the absorptivity, the conductivity or the diffusivity change along the welding process up to the steady state consolidation.

Therefore, it is concluded that the power supplied for a simulated circular heat source and the one supplied for a real wobbling method is dependent on the relation between the circle and the wobble rings areas. Consequently, less power is needed for welding if wobbling technique is applied, avoiding problems as power limitation or too little laser spots. To sum up, the model used for this work has a direct industrial application as it allows to determine the magnitude of the seams generated by laser welding for Inconel 718 sheets.

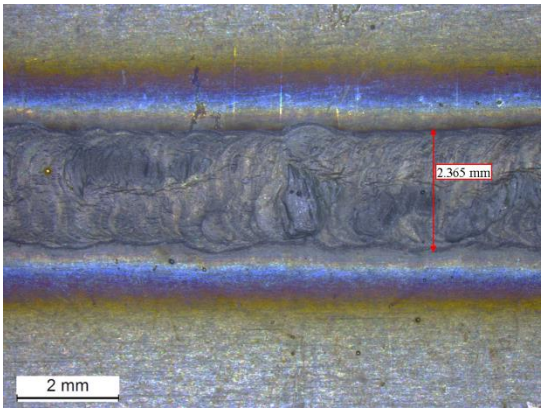

Fig. 6. Surface weld seam for 450 W and 5 $mm \cdot s^{-1}$ feeding speed.

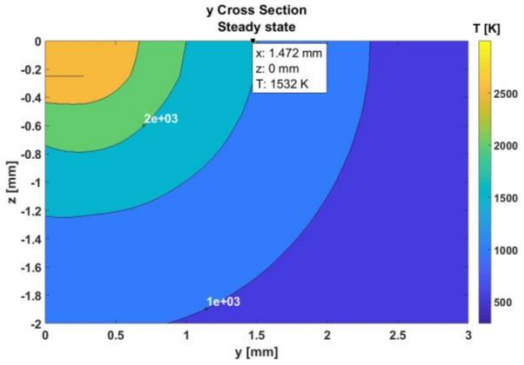

Fig. 7. Simulated weld cross section for 500 W and 3 $mm \cdot s^{-1}$ feeding speed.

Acknowledgements

Thanks are addressed to H2020-FoF13-2016 PARADDISE project (contract number 723440). Special thanks are addressed to the University of the Basque Country (UPV-EHU) for its financial support.

References

[1] Thakur A, Gangopadhyay S. State-of-the-art in surface integrity in machining of nickel-based super alloys, International Journal of Machine Tools and Manufacture, vol. 100; 2016. p. 25-54.
[2] Anderson M, Patwa R, Shin YC. Laser-assisted machining of Inconel 718with an economic analysis. International Journal of Machine Tools and Manufacture, vol. 46, no 14; 2006. p. 1879-1891.
[3] LIU, Sang, et al. Correlation of high power laser welding parameters with real weld geometry and microstructure. Optics & Laser Technology, vol. 94; 2017. p. 59-67.
[4] Ram GD, et al. Microstructure and tensile properties of Inconel 718 pulsed Nd-YAG laser welds. Journal of Materials Processing Technology, vol. 167, no 1; 2005. p. 73-82.

[5] Steen WM, Mazumder J. Laser material processing. Springer Science & Business Media; 2010. p. 201.
[6] Kazemi K, Goldak J. Numerical simulation of laser full penetration welding. Computational Materials Science, vol. 44, no 3; 2009. p. 841-849.
[7] Swift-Hook DT, et al. Penetration welding with lasers. Welding journal, vol. 52, no 11; 1973 p. 492-499.
[8] Dowden, J M. The mathematics of thermal modeling: an introduction to the theory of laser material processing. CRC Press, 2001.
[9] Haynes International (Kokomo, Indiana, USA). Inconel 718 product description.
[10] Wang H, et al. Effect of assist gas flow on the gas shielding during laser deep penetration welding. Journal of Materials Processing Technology, vol. 184, no 1-3; 2007. p. 379-385.
[11] Carlsaw HS, Jaeger JC. Conduction of heat in solids. Oxford: Clarendon Press, 2nd ed.; 1959.
[12] Römer G, De Graaf R. Direct calculation of optimized laser power density profiles for laser heating. En Proc. 15th Meeting on Modelling of Material Processing with Lasers (M4PL15); 2000.
[13] Römer G. Matlab Laser Toolbox User Manual. Version 0.1 beta. University of Twente, Faculty of Engineering Technology; 2010.
[14] Mills K.C. Recommended values of thermophysical properties for selected commercial alloys. Woodhead Publishing; 2002.
[15] Mazumder J, Laser Welding. In: Bass M (ed.). Laser materials processing. Elsevier; 1983.
[16] Mazumder J, Steen W.M. Heat transfer model for CW laser material processing. Journal of Applied Physics, vol. 51, no 2; 1980. p. 941-947.
[17] Klemens PG. Heat balance and flow conditions for electron beam and laser welding. Journal of Applied physics, vol. 47, no 5; 1976. p. 2165-2174.